Minimal and versatile description of diffusion and swelling in polymer-solvent systems: Modeling and experimental validation

Giuseppe Porpora [1,*] Andrea Gabriele [2] Raffaele Pastore [1] and Francesco Greco [1]

[1]*Department of Chemical, Materials and Production Engineering, University of Naples Federico II, P.le Tecchio 80, Napoli 80125, Italy*

[2]*The Procter and Gamble Company, Brussels Innovation Center, 1853 Strombeek Bever Temselaan 100, 1853 Grimbergen, Belgium*

(Received 12 May 2023; accepted 20 October 2023; published 13 November 2023)

The interplay between solvent diffusion and swelling of the absorbing solid leads to a variety of possible behaviors. In the case of polymer matrices, sharp penetration and swelling fronts are commonly found, with their dynamics depending on the specific features of the polymer-solvent system. Here, at the continuum mechanical level, we introduce a model to predict both concentration profile and swelling for whatever motion of the penetration front, in the one-dimensional case. A distinctive feature of our approach is that a constitutive equation for the thermodynamics of the dry side is not required. The model is validated against paradigmatic experiments available in literature, as well as through our own data (including optical microscopy) on a water–polyvinyl alcohol system. In spite of using only a small number of parameters, the model succeeds in predicting all the tested observables of the diffusion/swelling process in those polymeric systems.

DOI: 10.1103/PhysRevMaterials.7.115602

I. INTRODUCTION

Whenever a solvent is put in contact with a solid, *absorption* occurs. If the solid is endowed with some flexibility, absorption of solvent often causes a significant volume increase, the so-called *swelling* [1]. The interplay between solvent diffusion and solid deformation can originate a range of peculiar phenomena for the overall system [2]. When the solid is an initially dry polymer matrix, which is the case of interest here, the process frequently occurs with the emergence of two sharp fronts [3–6]. The first one is the contact surface between pure solvent and the hydrated side of the film, and is termed the *swelling* front. The second one is the boundary of solvent penetration at a given time: beyond it, the solid can be considered still dry. This second boundary is usually termed *hydration* (or *penetration*) front. The moving macroscopic hydration front corresponds, at a microscopic scale, to the solvent concentration profile showing a steep drop-down to zero that moves with time.

Figures 1(a)–1(c) show a top view of the absorption process of water in a polyvinyl alcohol (PVA) film, and of the ensuing swelling, as obtained by means of optical microscopy experiments (see below for details, Sec. III C). Three zones are clearly distinguishable, from left to right: water (white), the hydrated part of the film (black), and dry PVA (grayish). These three areas are sharply distinct, with moving swelling and hydration fronts being easily identified. Many experiments have been performed over the years on a wealth of polymer-solvent systems, with analogous qualitative features as in Fig. 1 in terms of fronts' presence and motion [7,8], but with a range of different quantitative features.

Commonly, the position of the hydration front as a function of time is well approximated by a power law. The exponent of such power law categorizes the type of diffusion for the given polymer-solvent system [9]. The term "Case I" diffusion is used to indicate a hydration front motion proportional to $t^{1/2}$ (which is the typical time dependence in purely diffusive processes), as opposed to "Case II" diffusion, indicating a hydration front advancing with a constant velocity, i.e., with a motion linear in time. Case I and Case II are just limiting scenarios, however, as systems in which the position of the hydration front is proportional to t^n, with $n \in]0.5, 1[$, are often observed, a situation usually named *anomalous* diffusion [10,11]. In the two limiting cases, for what matters the swelling front, some authors [12,13] report that it shares the same time dependence as the hydration front.

Notice that, apart from the nature of the given solvent-polymer system, the emergence of a certain type of transport will also depend on other factors affecting polymer relaxation or solvent motions, e.g., chain orientation [8], film thickness [14], and temperature [15]. Departure from "standard" Case I diffusion is often observed when the polymer relaxation rate is comparable with (or larger than) the diffusion rate [2].

The process of absorption/swelling in polymer matrices is of primary interest in several industrial applications, such as degradation and reprocessing of thermosetting polymers, or, for physical networks, healing and wet adhesion [16,17]. This latter example recently raised considerable interest in the design of polymer-based adhesives [18]. A liquid solvent, indeed, can soften the adherent's surface while preserving network existence, and promotes molecular mobility of polymer chains and the subsequent interdiffusion across the interface.

Due to the increasing relevance of such applications and to the scientific challenges underlying the process itself, interest in the subject is ample, and the relevant literature is quite rich. Several theoretical models have been developed over the

*giuseppe.porpora@unina.it

years to predict the evolution of swelling and of the solvent concentration profile [2,10,19], the most famous—and quite successful one—undoubtedly being the Thomas and Windle (TW) model [13,20]. The TW model is broad in scope, coupling chemical potential gradient with time-dependent mechanical deformation; it is also quite flexible, as in fact it can predict both Case I and Case II behaviors. Such a generality, however, comes at the cost of a high number of needed parameters; moreover, a nonstandard thermodynamic framework is perforce needed. Indeed, it should be remarked that, in TW theory (and in its successive extensions [21–23]), the solvent chemical potential is assumed to be directly dependent on a variable of evolution, i.e., the time derivative of concentration, and this peculiar choice requires in-depth analysis to possibly avoid problems of thermodynamic consistency. Overcoming such uncertainties in the TW approach is in fact a key motivation for the development of our own model.

Other previous efforts to circumvent these problems include a more basic theoretical approach [2] to the absorption/swelling process. The existence of a sharp hydration front is assumed *a priori*, and the motion of the front is either calculated via an *ad-hoc* "constitutive equation" for its velocity [24–26], or is *implicitly* given [2], or *directly* measured [12]. A critical issue arising in these models, however, is that a standard thermodynamic characterization of the dry state is often unavailable, or even unattainable, e.g., if dealing with an out-of-equilibrium solid.

Due to the above discussed limitations for the available theoretical frameworks, modeling of the absorption/swelling process in polymer matrices is still an open issue. Hence, we here introduce (Sec. II) a model that is more versatile and robust than the state-of-the-art ones, being able to describe any type of diffusion (Case I, Case II, and anomalous) while requiring just a few parameters (possibly, the *minimum* number of parameters), all of them being independently measurable. The predictions of this model are then validated (Sec. III) through both experimental data available in literature and our own experiments on a PVA–water mixture. Some conclusions are then given in the last section of the paper.

II. MODEL

Our model requires as an input the position of the hydration front measured as a function of time, thus falling in the same category as the approaches in Refs. [12,24,25]. To mathematically describe and justify this sharp front, the diffusion coefficient, exponentially increasing with solvent concentration (as is quite often observed [27]) in the hydrated side, is assumed to undergo a sudden jump to a constant, much lower, value beyond the front.

The equations of the model are presented here for the one-dimensional case, in a peculiar set of *non-Eulerian coordinates*, with the origin $X = 0$ always anchored to the swelling front, which proves to be convenient from the mathematical point of view. In a laboratory-fixed frame of reference, indeed, the integration domain will change with time on both hydration and swelling sides, in ways to be determined. The choice of the X set of coordinates, instead, allows one to deal with a single unknown, the overall extent of the hydrated part. The new coordinate X is related to the *Eulerian* coordinate x

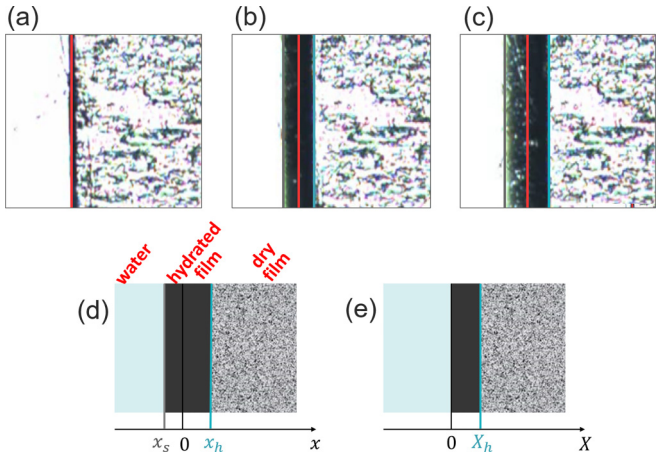

FIG. 1. Panels [(a)–(c)]: Three subsequent frames from a typical optical microscopy video for the absorption/swelling process in a PVA–water system. Initial condition (dry film) (a), $t = 5$ s (b), and $t = 10$ s (c). Black stripe is the hydrated portion of the film. Red line is the initial interface; light-blue and gray lines are hydration and swelling fronts, respectively. Panels (d) and (e): For a given time, representation of the absorption/swelling phenomenon in Eulerian (d) and non-Eulerian (e) coordinates.

through the (one-dimensional) deformation gradient $\lambda \equiv \frac{dx}{dX}$; the field $\lambda(X, t)$ is the local film stretching, to be determined. The second row of Fig. 1, panels (d) and (e), schematically shows the hydration phenomenon at a given time in the two different sets of coordinates, with the three zones solvent, hydrated, and dry from left to right. Notice that, in the X coordinate, the hydrated domain is "distorted" with respect to its laboratory-fixed shape.

In the X-coordinate description, the solvent mass balance for the hydrated side (side 1) reads as [12,28,29]

$$\frac{\partial C}{\partial t} = -\frac{\partial J}{\partial X} = -\frac{\partial}{\partial X}\left(-\frac{D(C)}{k_B T}\frac{C}{\lambda^2}\frac{\partial \mu}{\partial X}\right), \tag{1}$$

where $C = C(X, t)$ is the number concentration of solvent, J is the corresponding solvent flux, $D(C)$ is a diffusivity, which can change with concentration, μ is the solvent chemical potential, and $k_B T$ is the Boltzmann factor. The adopted constitutive equation for J in the X coordinate is standard, for an incompressible mixture, in the framework of irreversible thermodynamics, where a (local) linear relation between the flux and the thermodynamic force (i.e., the chemical potential gradient) is usually assumed [30,31].

A further constitutive equation for μ is now needed. Flory-Rehner model equations are here assumed to hold, not only at equilibrium, but also *instantly* and *locally*, with the as yet unknown one-dimensional fields $C(X, t)$ and $\lambda(X, t)$ defined at any elementary volume of the mixture. Notice that the adoption of Flory-Rehner theory is here made to describe the case of a hydrated network, and implies the absence of free volume inside the mixture, with any of the "lattice cells" being occupied by either a network monomer or a water molecule. Thus, the total volume of the mixture is given, at any time, as the sum of the volume of the dry polymer matrix and the absorbed solvent volume. Coherently, the two unknown fields are related by the incompressibility condition $\lambda = 1 + \nu C$,

thus giving μ as a function of C only [31]:

$$\frac{\mu}{k_B T} = \ln\left(\frac{\nu C}{1+\nu C}\right) + \frac{1}{1+\nu C} + \frac{\chi}{(1+\nu C)^2} + N\nu\left(1+\nu C - \frac{1}{1+\nu C}\right) \tag{2}$$

with ν the solvent molecule volume, χ the Flory polymer-solvent interaction parameter, and N the number density of polymer subchains. Two main contributions can be distinguished in Eq. (2): the first three terms in the right-hand side, indeed, represent the chemical potential due to the mixing of the molecules of polymer and solvent (in the limit of an infinite polymerization degree); the last term in the right-hand side, instead, takes into account network stretching.

In the dry side (side 2), where the matrix is essentially a solid (maybe even an out-of-equilibrium one) and water diffusion is highly hindered, thermodynamic constitutive equations are not used at all, and a classical Fickian diffusion is instead simply assumed, with a constant diffusion coefficient D_{02}. We remark that such a distinctive feature of our approach is of great importance, as (i) it avoids thermodynamic consistency issues; and (ii) it allows for dealing with a "dry" side that can be either at thermodynamic equilibrium (as is the case in [12]) or in an "arrested state," e.g., a glass, as in the TW case [20].

The complete problem can be thus described through a system of two partial differential equations:

$$\frac{\partial C}{\partial t} = D_{01}\frac{\partial}{\partial X}\left[e^{M\nu(C-C_{eq})}\xi(C)\frac{\partial C}{\partial X}\right],$$
$$\frac{\partial C}{\partial t} = D_{02}\frac{\partial^2 C}{\partial X^2} \tag{3}$$

[where $\xi(C) = \frac{C}{k_B T \lambda^2}\frac{\partial \mu}{\partial C}$; see Eqs. (1) and (2)], with the diffusivity on the hydrated side being

$$D(C) = D_{01} e^{M\nu(C-C_{eq})}. \tag{4}$$

Here, M is a positive dimensionless constant value, C_{eq} is the equilibrium concentration at the boundary of contact with pure water [see below, Eq. (5)], and D_{01} is a constant diffusivity, with $D_{01} \gg D_{02}$. In the dry region, it is $0 \leqslant C \leqslant C_h$, with C_h the concentration at the hydration front, X_h.

For the system of Eqs. (3), boundary conditions are as follows. At $X = 0$, i.e., at the swelling front, the constant concentration C_{eq} is obtained by imposing $\mu = 0$ in Eq. (2), with zero taken as the chemical potential of pure water:

$$\ln\left(\frac{\nu C_{eq}}{1+\nu C_{eq}}\right) + \frac{1}{1+\nu C_{eq}} + \frac{\chi}{(1+\nu C_{eq})^2} + N\nu\left(1+\nu C_{eq} - \frac{1}{1+\nu C_{eq}}\right) = 0. \tag{5}$$

At $X \to +\infty$ the slab will be considered dry at any time, $C = 0$. C_h is instead unknown, but it will be determined as a model output, from the fulfillment of the solvent mass balance across the hydration front: $[D(C)\xi(C)\frac{\partial C}{\partial X}]|_{X=X_h^-} = D_{02}\frac{\partial C}{\partial X}|_{X=X_h^+}$. The boundary conditions to be applied are thus

$$C(X = 0, t \geqslant 0) = C_{eq},$$

$$C(X = X_h(t), t \geqslant 0) = C_h(t) \tag{6}$$

for the hydrated side, and

$$C(X = X_h(t), t \geqslant 0) = C_h(t),$$
$$C(X \to +\infty, t \geqslant 0) = 0 \tag{7}$$

in the dry side. Notice that, in these boundary conditions, concentration at the hydration front will in general depend on time.

By solving the system of Eqs. (3) with boundary conditions (6) and (7), the entire concentration profile is obtained, as a function of time and space. The model can then be fully validated if the concentration profile is also experimentally accessible. Such a measurement, however, is not always straightforward, especially if the absorption/swelling process of interest is a rapid one. To validate the model, therefore, it proves useful to also compute integral quantities, easily accessed in experiments, such as the volume increase of the film and the total absorbed mass of solvent. Indeed, the readily measured swelling distance x_s (see Fig. 1) can be related to an integral of the C field:

$$|x_s(t)| = \int_0^{X_h(t)} [1 + \nu C(X,t)]dX - X_h(t). \tag{8}$$

Also, since volume additivity is assumed, the total absorbed solvent mass is obtained by a product of $|x_s|$ times the density of pure solvent. An indirect model validation will then be always available.

III. RESULTS

In this section, we will illustrate how our model proves to correctly predict not only the two limiting scenarios of Case I and Case II diffusion, but also anomalous diffusion. To this purpose, the diffusion/swelling behavior of three different polymer-solvent systems has been analyzed: chitosan/water, poly(methyl methacrylate) (PMMA)/methanol and PVA/water. For the first two systems, which exhibit Case I and Case II diffusion, respectively, the study has been conducted relying on literature data [12,13]; for the PVA/water mixture, instead, we here present our own experimental data. Solvent concentration profiles will be shown for the three cases, and model validation will be carried out by comparing the obtained predictions of swelling and absorbed mass of solvent with experimental data.

A. Case I diffusion

As an example of Case I diffusion, we focus on the case of water diffusing in a chitosan-based polymeric network. For this system, the predictions of our model are shown in Fig. 2 and compared with the results by Mao *et al.* [12]. The best fit ($9.31t^{0.5}$ μm, with t in seconds) obtained by Mao *et al.* for the hydration front is shown, as a dashed line, in Fig. 2(a). This time law has been used as an input for the solution of our equations. Circles are, instead, Mao *et al.* experimental data for swelling, and the solid black line is our model prediction for $x_s(t)$. The quite good agreement with experiments has been obtained using a *constant* diffusion coefficient in the hydrated side ($D_1 = D_{01}$, $M = 0$).

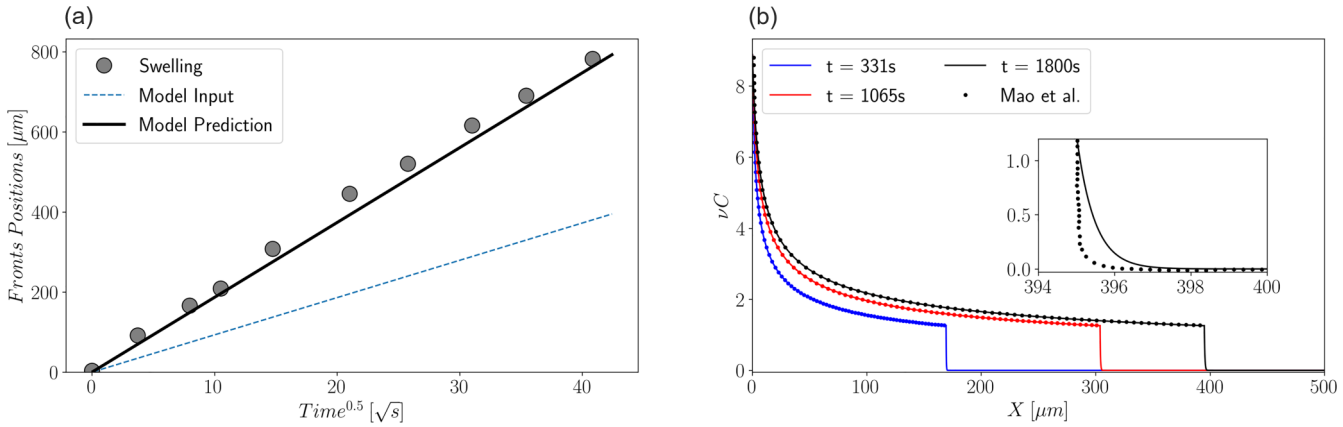

FIG. 2. Absorption/swelling process for a water-chitosan system. Panel (a): data (symbols) and our model predictions for the swelling front. Dashed line is a fit from [12] to the experimental data for the hydration front, used as an input for our model; solid line is the model prediction for the swelling front. Panel (b): comparison between predicted concentration profiles from our model (lines) and from the Mao *et al.* model [12] (symbols), at three times. In the inset, situation at the hydration front is shown, at $t = 1800$ s.

Figure 2(b) displays νC vs X, at various times, as calculated both by Eqs. (3) (lines) and by the Mao model [12] (symbols). The differences in the calculated profiles in the dry side are highlighted in the inset, where it is apparent that the standard Fickian diffusion (our model) shows a smoother profile as compared to the one obtained by the Mao model. Interestingly, despite these differences, the concentration C_h that guarantees mass conservation across the hydration front is the same between the two models, and is always independent from time, resulting in identical solvent concentration profile predictions in the hydrated region. All the needed parameters for our model are taken from Ref. [12]: $\chi = 0.41$, $N = 4.27 \times 10^{24}$ m^{-3}, and $D_{01} = 5.15 \times 10^{-9}$ m^2/s, $D_{02} = 5.15 \times 10^{-14}$ m^2/s. It is here worth emphasizing again, however, that in the Mao model further parameters were needed for the thermodynamic description of the dry side, which is instead avoided in our approach.

B. Case II diffusion

The system chosen as an example of Case II diffusion is liquid methanol in glassy PMMA, the one studied in the seminal paper by TW [13,20], a system which still gains much interest nowadays [32].

Figure 3(a) shows the original measurements for the positions of the hydration and swelling fronts as a function of time. The best linear fit for those hydration data [dashed line: $(6.0 \pm 0.1)t$ μm, with t in hours] has been here used for our model input, and the solid black line is the model prediction for $x_s(t)$ via Eq. (8), in good agreement with data. In the original paper, measurements of concentration profiles and absorbed methanol mass as a function of time are also available. Figure 3(b) shows the predicted νC vs X for five different times (lines), and a comparison with the measured concentration profile after 60 h of diffusion. Agreement with data is excellent. It is worth noticing that, in this system, the concentration C_h at the hydration front slightly decreases with time. In the rightmost panel of Fig. 3, the predicted absorbed mass of solvent is shown (line), together with the experimental data. For all the considered quantities (swelling, concentration profile, and absorbed mass), the agreement between data and our predictions is quite good. It is worth noting that our predictions have been obtained assuming an exponential diffusion coefficient $M = 28$, a value well within the M range estimated by TW. Other parameters are $\chi = 1$, $N = 3.5 \times 10^{27}$ m^{-3}, $D_{01} = 5 \times 10^{-12}$ m^2/s, and $D_{02} = 10^{-14}$ m^2/s, all of them taken from the original TW paper. Once again, we emphasize that the parameters needed in our computation (χ, N, D_{01}, M, and D_{02}) are fewer than in the original TW work.

C. Anomalous diffusion

Now we show how our model can successfully describe the anomalous diffusion observed in our experiments for a (solvent-casted) PVA physical network in water. PVA is a hydrophilic, synthetic polymer, nontoxic and biocompatible, widely used for several industrial applications [33–36]. Notice that, since the PVA film in our experiments is in a rubbery state, the absorption/swelling process is very fast: we then limit our analysis to 5 s only [37]. The experimental setup to measure the positions of hydration and swelling fronts is composed by two Perspex plates (5 cm × 5 cm) held together by magnets, with a small PVA sample (1 cm × 1 cm, thickness 76 μm) sandwiched in between. The top plate is pierced, thus allowing for water application via a 15-ml pipet. The process is observed with a Zeiss Axiovert 200 microscope (reflection mode), using a magnification of 2.5×, and recorded. An example of such recordings is in Fig. 1. Full details on the setup and on the front-tracking procedure and codes will be given elsewhere.

Figure 4(a) gives the positions of hydration and swelling fronts in time, as obtained by performing image analysis on the recorded videos. Power-law fits for the fronts' positions in time are $(8.5 \pm 0.1)t^{0.64 \pm 0.01}$ for the hydration front and $(12.6 \pm 0.1)t^{0.55 \pm 0.01}$ for the swelling one, classifying the diffusion as anomalous. As before, we use the (fitted) hydration front evolution as the input, and obtain $x_s(t)$ from our model, in excellent agreement with data. The panel (b) of Fig. 4 shows the predicted concentration profiles at various times. It is interesting to note the huge difference in the shape of

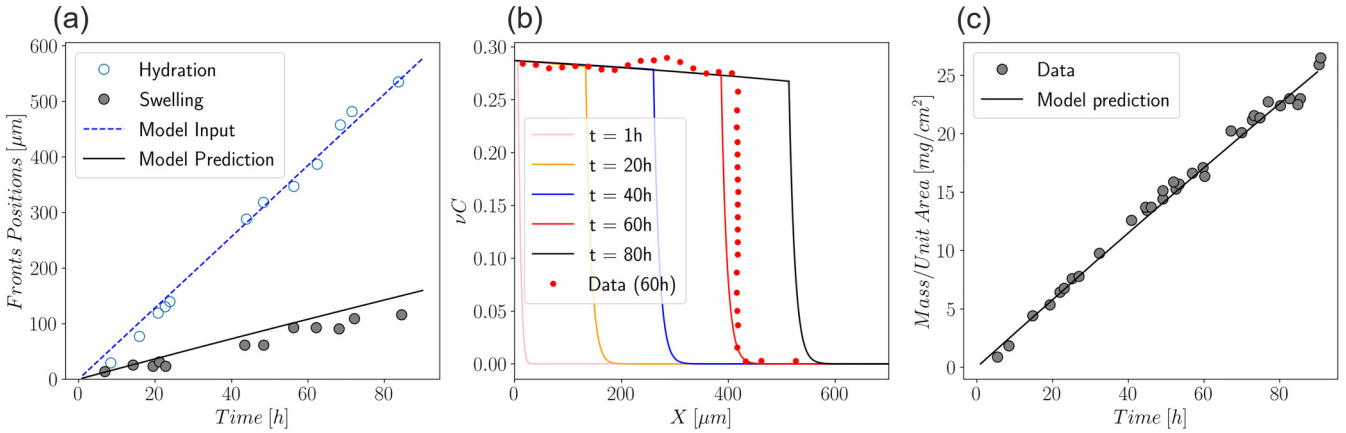

FIG. 3. Absorption/swelling process for a methanol-PMMA system. Panel (a): data for hydration and swelling fronts (symbols) and our model predictions for the swelling front (solid line). Dashed line is a linear fit (model input) for the hydration front. Panel (b): predicted concentration profiles at five times (lines); experimental data (symbols) at 60 h. Panel (c): measured (symbols) and predicted (line) total absorbed solvent mass as a function of time. All experimental data are taken from [13,30].

the predicted concentration profiles with respect to the previously examined TW case. Here, however, experimental data are lacking. In the inset, it is shown that, in this system as in the TW case, the concentration C_h at the hydration front decreases with time. In Fig. 4(c), the predicted absorbed mass of solvent is compared with the experimental data (obtained gravimetrically, by weighting the hydrated film at different times), and excellent agreement is again found.

For this system, a constant diffusivity has been chosen in the hydrated side, which we set as the self-diffusivity of water at room temperature: $D_{01} = 2.3 \times 10^{-9}$ m^2/s. For the polymer-solvent interaction parameter, the most common value found in literature for the water–PVA solutions at room temperature has been used: $\chi = 0.494$. The last parameter N [see Eq. (2)] does not show any significant impact on the predictions, at least over the time span we are interested in here. To obtain our results, $N = 10^{24}$ m^{-3} has been chosen as a reasonable value [12,28]. As a perspective, a value for N could be separately estimated from the approximate relation $G \approx Nk_BT$, where the polymer elastic modulus G can be measured, for example, through dynamic mechanical analysis.

IV. CONCLUSIONS

In this work, a "minimal" model to describe liquid diffusion and swelling in polymer films has been introduced, and applied to predict the behavior of very different systems: water/chitosan, methanol/PMMA, and water/PVA. We find that a concentration-dependent diffusivity is needed to fit the data in the glassy system methanol/PMMA (Case II diffusion), whereas a constant diffusion coefficient in the hydrated side of the medium suffices to describe Case I and anomalous diffusion. The accuracy of our model and its flexibility are quite remarkable, since results are obtained by only exploiting basic Flory-Rehner thermodynamics for the hydrated side,

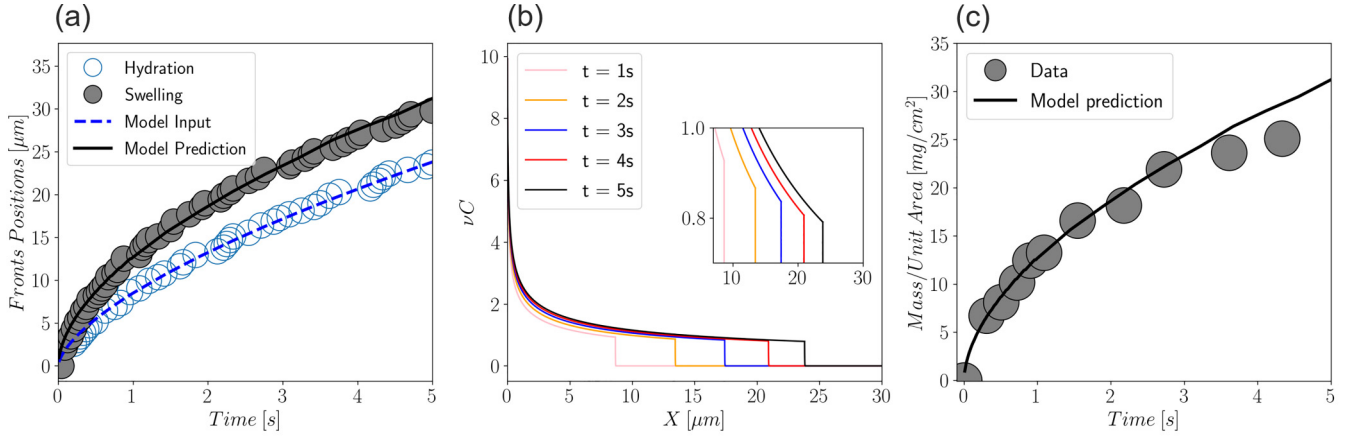

FIG. 4. Absorption/swelling process for a water–PVA system. Panel (a): Data for hydration and swelling fronts (symbols) and our model predictions for the swelling front (solid line). Dashed line is a power-law fit (model input) for the hydration front. Panel (b): Predicted concentration profiles at five times (lines). In the inset, the prediction of a C_h decrease in time is given. Panel (c): Measured (symbols) and predicted (line) total absorbed solvent mass as a function of time. All experimental data are original; symbols size represents the maximum standard deviation upon five repetitions of the experiment.

and a thermodynamics-free description for the dry side, which leads to a relatively small number of needed parameters, as compared to other models. It is also worth emphasizing here that those parameters are all measurable, in principle at least, in independent experiments.

Overall, we believe that insights in this work arise from a simplifying and in fact more far-reaching change in the constitutive equation for the dry side (diffusivity is all that is needed), as well as from pointing out the difficulties possibly hidden in the adoption of a "quasi"-thermodynamical constitutive equation (TW). Further assessment of the model validity will of course require other experiments. To this purpose, we want to mention that we are currently collecting many further experimental results in various water–PVA systems. Our preliminary results are in full agreement with predictions of the model introduced here.

[1] T. L. Hill, *An Introduction to Statistical Thermodynamics* (Courier Corporation, Chelmsford, MA, 1986).

[2] J. Crank, *The Mathematics of Diffusion* (Oxford University Press, New York, 1979).

[3] G. S. Hartley, Trans. Faraday Soc. **42**, B006 (1946).

[4] G. S. Hartley, Trans. Faraday Soc. **45**, 820 (1949).

[5] C. Robinson, Trans. Faraday Soc. **42**, B012 (1946).

[6] T. K. Kwei and H. M. Zupko, J. Polymer Sci. Part A-2: Polym. Phys. **7**, 867 (1969).

[7] J. H. Petropoulos and M. Sanopoulou, J. Polym. Sci., Part B: Polym. Phys. **26**, 1087 (1988).

[8] M. Sanopoulou and J. H. Petropoulos, J. Polym. Sci., Part B: Polym. Phys. **30**, 983 (1992).

[9] T. Alfrey Jr., E. F. Gurnee, and W. G. Lloyd, J. Polym. Sci., Part C: Polym. Symp. **12**, 249 (1966).

[10] D. Vesely, Int. Mater. Rev. **53**, 299 (2008).

[11] We here highlight that, in this entire work, the absorption/swelling problem is addressed only via continuum mechanics, where the expression *anomalous diffusion* assumes the just described meaning. The reader should thus not be confused with the same term being used in the microscopic approach to diffusion, where it refers to a mean square displacement that is nonlinear in time.

[12] X. Mao, H. Yuk, and X. Zhao, J. Mech. Phys. Solids **137**, 103863 (2020).

[13] N. Thomas and A. H. Windle, Polymer **19**, 255 (1978).

[14] C. J. Durning and W. B. Russel, Polymer **26**, 131 (1985).

[15] A. Windle, *Polymer Permeability* (Springer, New York, 1985), pp. 75–118.

[16] Q. Shi, K. Yu, M. L. Dunn, T. Wang, and H. J. Qi, Macromolecules **49**, 5527 (2016).

[17] Q. Wang, J. L. Mynar, M. Yoshida, E. Lee, M. Lee, K. Okuro, K. O. Kinbara, and T. Aida, Nature (London) **463**, 339 (2010).

[18] C. Cui and W. Liu, Prog. Polym. Sci. **116**, 101388 (2021).

[19] S. Bargmann, A. T. McBride, and P. Steinmann, Appl. Mech. Rev. **64**, 010803 (2011).

[20] N. L. Thomas and A. H. Windle, Polymer **23**, 529 (1982).

[21] C. J. Durning, J. Polym. Sci., Polym. Phys. Ed. **23**, 1831 (1985).

[22] C.-Y. Hui, K.-C. Wu, R. C. Lasky, and E. J. Kramer, J. Appl. Phys. **61**, 5129 (1987).

[23] C.-Y. Hui, K.-C. Wu, R. C. Lasky, and E. J. Kramer, J. Appl. Phys. **61**, 5137 (1987).

[24] G. Rossi, P. A. Pincus, and P.-G. De Gennes, Europhys. Lett. **32**, 391 (1995).

[25] G. Astarita and G. C. Sarti, Polym. Eng. Sci. **18**, 388 (1978).

[26] M. R. Foreman and F. Vollmer, Phys. Rev. Lett. **114**, 118001 (2015).

[27] M. Sanopoulou, D. F. Stamatialis, and J. H. Petropoulos, Macromolecules **35**, 1012 (2002).

[28] W. Hong, X. Zhao, J. Zhou, and Z. Suo, J. Mech. Phys. Solids **56**, 1779 (2008).

[29] L. D. Landau and E. M. Lifshitz, *Fluid Mechanics: Landau and Lifshitz: Course of Theoretical Physics* (Elsevier, New York, 2013), Vol. 6.

[30] F. P. Duda, A. C. Souza, and E. Fried, J. Mech. Phys. Solids **58**, 515 (2010).

[31] S. A. Chester and L. Anand, J. Mech. Phys. Solids **58**, 1879 (2010).

[32] J. Nixdorf, G. Di Florio, L. Broöckers, C. Borbeck, H. E. Hermes, S. U. Egelhaaf, and P. Gilch, Macromolecules **52**, 4997 (2019).

[33] N. Krishna and F. Brow, Am. J. Ophthalmol. **57**, 99 (1964).

[34] R. Abedi-Firoozjah, N. Chabook, O. Rostami, M. Heydari, A. Kolahdouz-Nasiri, F. Javanmardi, K. Abdolmaleki, and A. M. Khaneghah, Polym. Test. **118**, 107903 (2022).

[35] M. I. Baker, S. P. Walsh, Z. Schwartz, and B. D. Boyan, J. Biomed. Mater. Res., Part B **100B**, 1451 (2012).

[36] D. Zhang, W. Zhou, B. Wei, X. Wang, R. Tang, J. Nie, and J. Wang, Carbohydr. Polym. **125**, 189 (2015).

[37] On such a short timescale, edge effects in the process are safely negligible.